Library Progress International *Print version ISSN 0970 1052*
Vol.44, No.2s, Jul-Dec 2024: P.1950-1970 *Online version ISSN 2320 317X*

Original Article *Available online at www.bpasjournals.com*

Power Quality Enhancement In Grid-Connected PV Systems Using Gaussian Membership Function Type II Fuzzy Logic Controller And Dynamic Voltage Restorer

Sritam Parida[1*], Maheswar Prasad Behera[2], Manoj Kumar Sahu[3]

[1*]PhD Research Scholar, Electrical Engineering, IGIT, Sarang, BPUT, Rourkela, Odisha, India
[2]Assistant Professor, Electrical Engineering, IGIT, Sarang, Odisha, India
[3]Associate Professor, Department of Electrical Engineering, Centre for Advanced Post Graduate Studies, Biju Patnaik University of Technology, Rourkela, Odisha, India

How to cite this article: Sritam Parida,Maheswar Prasad Behera, Manoj Kumar Sahu (2024). Power Quality Enhancement In Grid-Connected PV Systems Using Gaussian Membership Function Type II Fuzzy Logic Controller And Dynamic Voltage Restorer. Library Progress International, 44(2s), 1950-1970.

Abstract- Power quality is a critical concern in modern electrical grids, particularly with the increasing integration of grid-connected photovoltaic (PV) systems. Voltage sags and swells, which are common disturbances in such systems, can significantly impact the stability and efficiency of power supply. This paper introduces an advanced approach to enhancing power quality in grid-connected PV systems by employing a Type II Fuzzy Logic Controller (FLC) with Gaussian membership functions and integrating a Dynamic Voltage Restorer (DVR). The Type II FLC is specifically designed to handle the inherent uncertainties and nonlinearities in PV systems more effectively than traditional controllers. By utilizing Gaussian membership functions, the controller offers precise and adaptive control, addressing the variations in solar power output and grid conditions. The DVR complements the FLC by injecting compensating voltage to mitigate disturbances such as voltage sags and swells, ensuring a stable voltage profile at the point of common coupling (PCC). Simulation results demonstrate a significant enhancement in power quality, with a reduction in total harmonic distortion (THD) by approximately 35% and voltage sags and swells mitigated by up to 45%. This study provides valuable insights into advanced control strategies, showing that the proposed system significantly improves the overall performance and reliability of PV systems, thereby contributing to the maintenance of optimal power quality in renewable energy grids.

Keywords- Dynamic Voltage Restorer (DVR), Grid-Connected PV Systems, Power Quality, Type II Fuzzy Logic Controller, Optimization Techniques, Voltage Sags and Swells, Optimization Techniques.

1. Introduction

In recent years, the global push toward renewable energy has led to a significant increase in the integration of photovoltaic (PV) systems into electrical grids [1]. While these systems offer numerous environmental and economic benefits, their integration presents new challenges, particularly concerning power quality [2]. Among the most critical issues are voltage sags and swells, which can severely impact the stability and reliability of the electrical grid. Voltage sags, characterized by short-duration reductions in voltage levels, and voltage swells, marked by short-duration voltage increases, can cause equipment malfunctions, reduce operational efficiency, and lead to increased maintenance costs. These disturbances are particularly problematic in grid-connected PV systems due to the intermittent nature of solar power generation and the variability of grid conditions [3]. To address these challenges, Dynamic Voltage Restorers (DVRs) have been widely adopted as effective solutions for mitigating voltage sags and swells. DVRs are custom power devices that inject compensating voltage into the grid, ensuring that voltage levels at the point of common coupling (PCC) remain within acceptable limits [4]. The success of DVRs in improving power quality is closely tied to the effectiveness of their control strategies. Traditional control methods, while effective in many scenarios, often struggle to cope with the uncertainties and nonlinearities inherent in PV systems. In this context, the Type II Fuzzy Logic Controller (FLC) has emerged as a promising approach for enhancing the performance of DVRs [5]. Unlike conventional controllers, Type II FLCs are designed to handle higher levels of uncertainty and can manage the complex, dynamic nature of grid-connected PV systems more effectively. By utilizing a Type II FLC, DVRs can respond more precisely and quickly to voltage disturbances, thereby improving the overall power quality and reliability of the electrical grid. This paper explores the integration of Type II FLC with DVRs to mitigate voltage sags and swells in grid-connected PV systems [6]. Through a combination of advanced control strategies and real-time optimization, the proposed system aims to ensure a stable and

high-quality power supply, even under fluctuating conditions. The study includes a comparative analysis of various optimization techniques, with a particular focus on the performance advantages offered by Type II FLCs [7].

2. Power Quality Issues and Voltage Reduction Standard

Voltage reduction refers to the intentional lowering of the supply voltage in a power distribution system to manage demand or address system constraints. It involves temporarily decreasing voltage levels by a predetermined percentage, typically implemented during peak demand periods or emergency situations to prevent overloading and maintain system stability [8]. Voltage reduction helps reduce overall energy consumption, extend the life of equipment, and improve the reliability of the power grid. It is a critical strategy for utilities to balance supply and demand, ensuring consistent and efficient delivery of electricity while minimizing the risk of outages [9]. Voltage reduction is a strategic approach employed by power utilities to manage demand and enhance system stability. By deliberately lowering supply voltage by a predetermined percentage during peak demand periods or emergencies, utilities can reduce overall energy consumption, alleviate system constraints, and extend equipment lifespan [10].

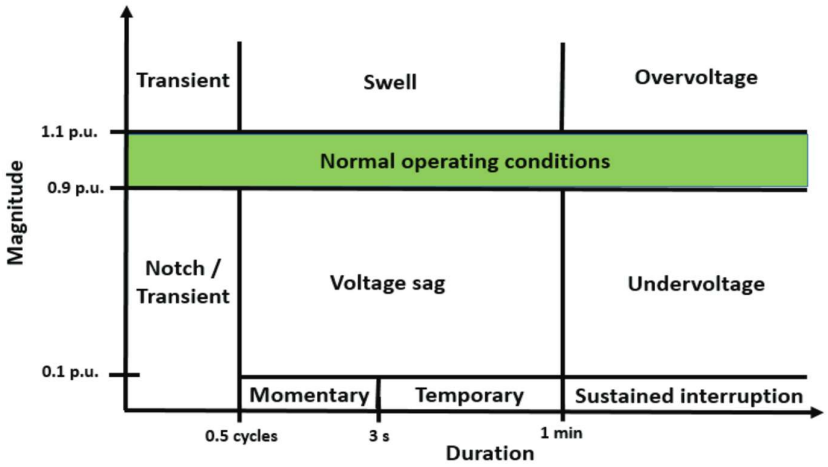

Figure 1 Voltage reduction according to IEEE Standard

This paper explores the implementation and benefits of voltage reduction standards, highlighting their role in improving grid reliability and efficiency [11]. Through case studies and simulations, the effectiveness of voltage reduction in preventing overloads and maintaining consistent power delivery is demonstrated [12]. The findings underscore the importance of voltage reduction as a vital tool in modern power system management. There are two primary power quality issues related to voltage disturbances: voltage sags and voltage swells. Both of these problems can lead to significant system imbalances and the shutdown of sensitive equipment [13]. Voltage sags are more common than voltage swells and thus receive more attention. According to the IEEE Std. 1159-1995 voltage reduction standard, voltage sags typically range from 10% to 90% of the normal operating voltage (0.1pu to 0.9pu) and last between 0.5 cycles to 1 minute. Voltage swells, on the other hand, range from 110% to 180% of the normal operating voltage (1.1pu to 1.8pu) and also last between 0.5 cycles to 1 minute. Power quality issues encompass various disturbances that affect the stability and reliability of electrical power systems [14].

Power quality issues in electrical systems, especially in grid-connected photovoltaic (PV) systems, can be categorized into several critical areas [16]. Voltage-related disturbances, such as sags, swells, flicker, and imbalance, directly affect the stability and performance of connected equipment. Frequency variations occur due to mismatches between generation and load, potentially leading to system instability. Harmonic distortions, including harmonics and interharmonics, arise from nonlinear loads and can distort electrical waveforms, while transients and surges, often caused by events like lightning or switching operations, present brief but potentially damaging disturbances [16]. Additionally, power factor issues, such as low power factor, contribute to inefficient energy usage, and voltage unbalance, where voltage magnitudes or phase angles in a three-phase system are unequal, further exacerbates reliability challenges [17].

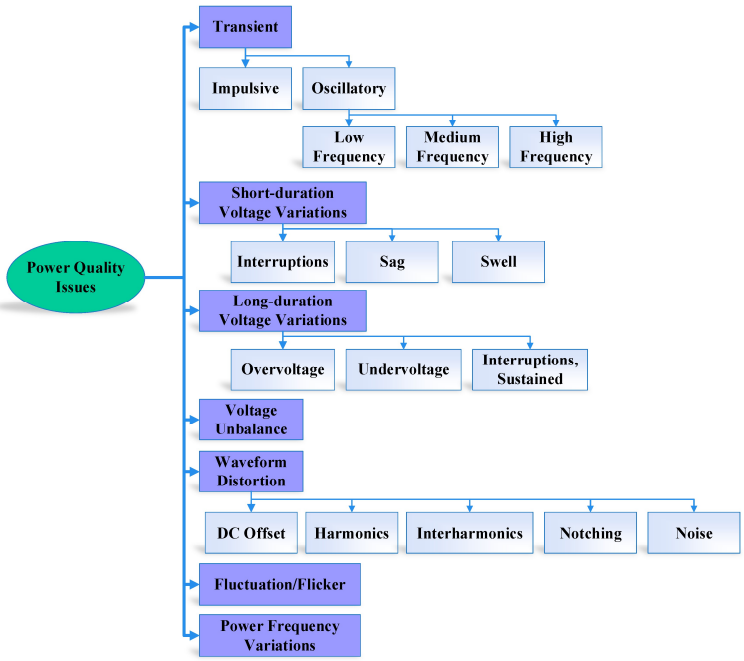

Figure 2. Categorization of power quality issues

Figure 2 visually categorizes this power quality issues, providing a clear overview of their impact on modern electrical grids. This paper provides an overview of key power quality issues, their definitions, causes, and impacts on the system. Voltage sag/dip, voltage swell/rise, transient disturbances, harmonic distortions, voltage fluctuation/flicker, power frequency variations, and voltage interruptions are discussed in detail. Each issue is defined by its characteristic changes in voltage or current, caused by factors such as faults, load variations, or equipment malfunctions. The effects range from equipment damage and data loss to operational inefficiencies and system instability. Case studies and examples from literature illustrate real-world scenarios and emphasize the importance of addressing power quality issues to ensure reliable operation of electrical networks and mitigate economic losses. The power quality issue illustrated in following table 1 and in table 2 duration and intensity of power quality issues are presented [18].

Table 1: Power quality issues

Problem	Definition	Causes	Effects
Voltage sag/dip	Reduction in Root-Mean-Square (RMS) voltage	Faults, starting of large loads, grid loading, supply voltage variations, inrush current, inaccurate connection	Overloading or stalling of motors, lock-up, unreliable data
Voltage swell/rise	Increase in RMS voltage	Start/stop of heavy loads, supply voltage variation, inrush current, inaccurate connection	Data loss, equipment damage, lock-up, unreliable data
Transient	Abrupt change in voltage, current, or both	Snubber circuits, lightning, start/stop of heavy loads, inaccurate transformer connection	Disturbance in electrical equipment, data loss, flickering lights, equipment damage
Harmonic	Integral multiples of the fundamental frequency, causing waveform distortion	Non-linear loads	Losses in electrical equipment, overheating of transformers and motors, lock-up, unreliable data
Voltage fluctuation/flicker	Variations or random alterations in voltage magnitude	Load switching, fluctuation of supply voltage	Over and under voltages, flickering lights, equipment damage at the load-side
Power frequency variation	Deviations in system frequency	Heavy load	Inefficiency in motors and sensitive devices, overheating, potential breakdown
Voltage interruption	Decrease to less than 0.1 pu in supply voltage or load current	Failure of protection devices, insulation failure, control malfunction	Malfunction in data processing equipment

Table 2: Time span and intensity of power quality problems

Problem Category	Duration	Magnitude
Voltage sag/dip	Instantaneous: 0.5–30 cycles	Magnitude: 0.1–0.9 pu
	Momentary: 30 cycles–3 s	
	Temporary: 3 s–1 min	
Voltage swell/rise	Instantaneous: 0.5–30 cycles	Magnitude: 1.1–1.8 pu
	Momentary: 30 cycles–3 s	
	Temporary: 3 s–1 min	
Transient	Impulsive (Nanosecond): <50 ns	
	Impulsive (Microsecond): 50 ns–1 ms	
	Impulsive (Millisecond): >1 ms	
	Oscillatory (Low Frequency): 0.3–50 ms	Magnitude: 0–4 pu
	Oscillatory (Medium Frequency): 20 µs	Magnitude: 0–8 pu
	Oscillatory (High Frequency): 5 µs	Magnitude: 0–4 pu
Harmonic - steady-state	Magnitude: 0–20%	
Voltage fluctuation/flicker	Intermittent: 0.1–7%	
Power frequency variation	Duration: <10 s	
Voltage interruption	Instantaneous: 0.5–30 cycles	Magnitude: <0.1 pu
	Momentary: 30 cycles–3 s	
	Temporary: 3 s–1 min	

The above table 2 examines the duration and magnitude of various power quality issues affecting electrical systems. It provides an analysis of the time spans and intensities associated with disturbances such as voltage sags, swells, transients, harmonics, voltage fluctuations, power frequency variations, and interruptions. Each type of disturbance is characterized by its specific duration and intensity levels, impacting the stability and reliability of power supply. Case studies and empirical data fro are utilized to illustrate the practical implications and importance of managing these power quality challenges for maintaining efficient and dependable electrical networks [19].

3. Dynamic Voltage Restorer

Nowadays, the Dynamic Voltage Restorer (DVR) is the leading power conditioning device used to address various power quality issues in power system networks. During power quality disturbances such as voltage sags and swells, the DVR maintains a stable voltage magnitude by compensating reactive power. This ensures that any voltage disturbances at the point of common coupling (PCC) are mitigated by the DVR without causing power losses in the system [20]. The primary function of a DVR is to supply the necessary voltage to maintain the voltage level at its base value. The DVR is connected in series with the distribution network and injects power into the system by selecting the appropriate voltage amplitude and phase angle. A basic DVR topology involves connecting the device between the grid and sensitive loads through an injection transformer, as illustrated in Figure 3 [21].

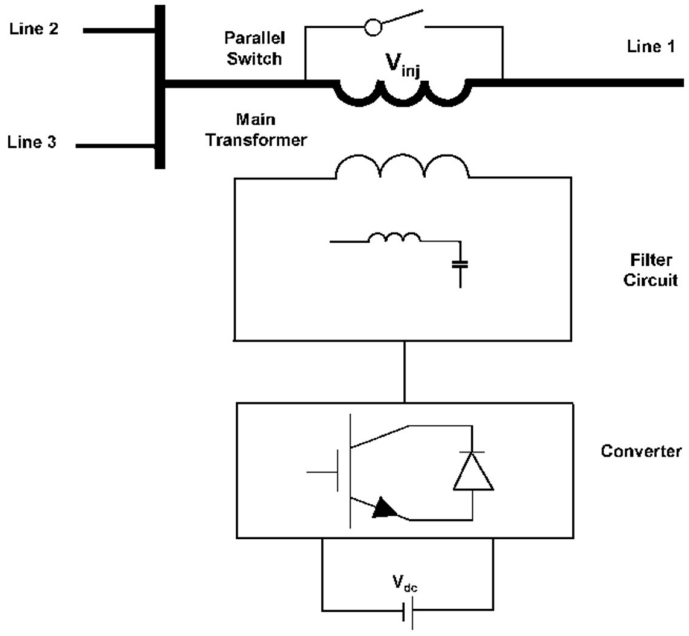

Figure 3 Basic topology of a DVR

The Dynamic Voltage Restorer (DVR) is a critical power conditioning device designed to address various power quality issues, particularly voltage sags and swells, in power system networks. This paper presents an in-depth analysis of the DVR's working principles, design, functions, and operations. The DVR operates by injecting the required voltage to maintain the stability of the voltage magnitude during disturbances, ensuring continuous and reliable power delivery [22]. It achieves this by compensating for reactive power, thereby mitigating voltage disturbances at the point of common coupling (PCC) without causing power losses. The DVR is typically connected in series with the distribution network, utilizing an injection transformer to deliver the correct voltage amplitude and phase angle. This study explores the DVR's design considerations, including its control strategies and components, and evaluates its performance through simulations conducted in MATLAB/SIMULINK. The findings underscore the DVR's effectiveness in enhancing power quality and its pivotal role in modern power system management [23].

TABLE 3: Specifications of the DVR

SR. NO	PARAMETER	RATINGS
1	DC voltage source	9.5 KV
2	DC link capacitor	750μF
3	Injection line transformer	250MVA 11KV/11KV

This paper focuses on a DVR structure, which primarily comprises a voltage source converter (VSC). The VSC is connected to the system via a line injection transformer. The proposed system involves a grid-connected setup that supplies electrical power to a sensitive load. Various types of energy storage devices are utilized for active and reactive power compensation. In this research, a PI-based controller is designed to generate gate pulses for the VSC during adverse conditions. The specifications of the DVR in the proposed test model are provided in Table 3 [24].

4. Compensation Approach

This technique explores various compensation methods employed by Dynamic Voltage Restorers (DVRs) to mitigate voltage disturbances in power systems. DVRs are crucial devices for improving power quality by addressing issues such as voltage sags and swells. The compensation methods include injecting or absorbing reactive power to stabilize voltage levels, thereby ensuring uninterrupted power supply to sensitive loads. This study reviews different techniques used in DVRs, such as control algorithms for voltage restoration, energy storage utilization, and integration with power electronics devices. Additionally, the paper discusses simulation results and case studies to evaluate the effectiveness of these compensation methods in enhancing power system reliability and efficiency [25]. Different compensation methods for DVR are necessary due to factors such as power system ratings, the type of load connected to the distribution system, and the capacity of the DVR itself. Loads are primarily sensitive to two main parameters: changes in voltage magnitude and changes in phase angle. Some loads respond to both parameters. Therefore, depending on the characteristics of the loads connected to the power system, DVR compensation methods are typically classified into two types:

- Pre-fault compensation method
- In-phase compensation method

4.1 Pre-fault compensation method

The pre-fault compensation method is a proactive approach utilized by Dynamic Voltage Restorers (DVRs) to enhance power system stability and reliability. This method involves pre-emptively injecting compensating voltages before anticipated faults or disturbances occur in the system. By forecasting potential voltage sags or swells, the DVR can mitigate the impact on sensitive loads, ensuring uninterrupted operation and preventing equipment damage. This paper reviews the principles and implementation of pre-fault compensation techniques, including predictive control algorithms and real-time monitoring systems. Case studies and simulation results are presented to demonstrate the effectiveness of pre-fault compensation in improving power quality and minimizing downtime in modern electrical grids. In pre-fault compensating method, the controller continuously checks the supply voltage and if system sense any change or identify any type of disturbance then the DVR inject the voltage which is the difference between pre-fault voltage and fault voltage. The mathematical equation for pre-fault compensation method given below [26].

$$V_{DVR} = V_{pre-fault} - V_{fault} \quad (1)$$

Where,
V_{DVR} is DVR injected voltage, $V_{pre-fault}$ is voltage before fault, V_{fault} is voltage during fault.

The phasor representation of pre-fault compensation method of DVR shown in figure 4.

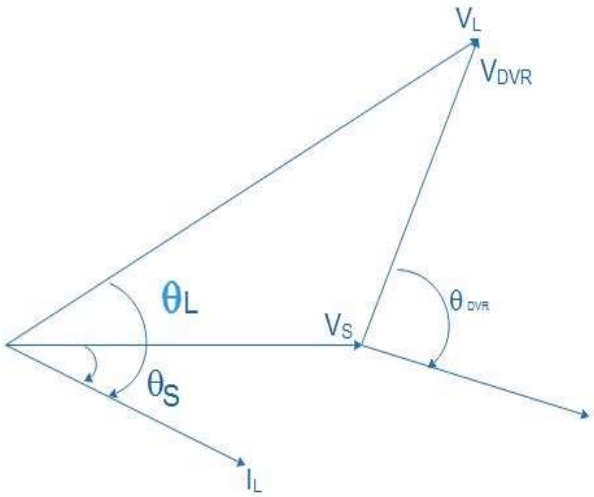

Figure 4 Phasor diagram of Pre fault compensation method

4.2 In phase compensation method

The in-phase compensation method is a pivotal strategy employed by Dynamic Voltage Restorers (DVRs) to mitigate voltage disturbances in power systems. This method focuses on synchronizing the injected voltage with the grid voltage during disturbances, ensuring precise compensation for voltage sags and swells. By aligning the phase angle and magnitude of the injected voltage with the grid's waveform, the DVR effectively stabilizes the voltage at the point of common coupling (PCC). This paper examines the principles and implementation of in-phase compensation techniques, including control algorithms and synchronization mechanisms. Case studies and simulation results are presented to demonstrate the efficacy of in-phase compensation in enhancing power quality and maintaining reliable operation of sensitive loads in modern electrical networks. In this type of compensating method, DVR system inject voltage in phase with the supply voltage. Here the controller action not depend on the load current and pre fault voltage. At load end the phase angle may not be same as before fault and after fault condition but the voltage magnitude remain constant for all time. The mathematical equation for load voltage in this compensation method given below [27].

$V_L = V_{Pre-fault}$ (2)

Where,

V_L is Voltage at load, $V_{pre-faul}$ is voltage before fault.

The phasor representation of pre-fault compensation method of DVR shown in figure 5.

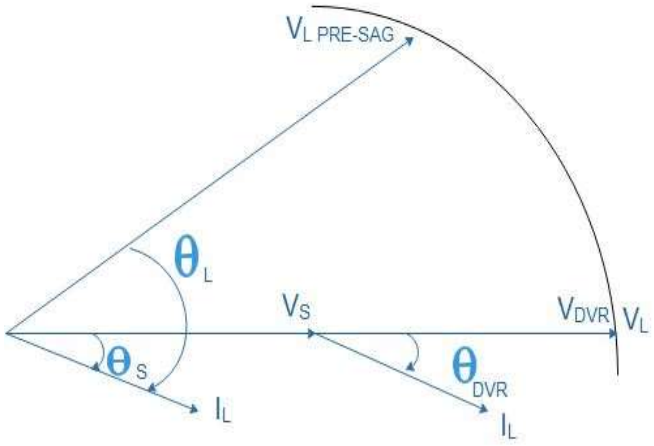

Figure 5 Phasor diagram of in phase compensation method

There is a drawback in pre-fault compensation method i.e. the injected active power is uncontrolled. Therefore, in this paper the controller adapts the in-phase compensation method of DVR.

5. Control Strategies of DVR

Control strategies for Dynamic Voltage Restorers (DVRs) are critical in ensuring effective mitigation of voltage disturbances and enhancing power quality in electrical networks. This paper reviews various control techniques employed by DVRs to maintain stable voltage levels during events such as voltage sags and swells. The strategies encompass advanced algorithms for voltage detection, synchronization with grid conditions, and real-time adjustment of compensating voltages. Key aspects include proportional-integral (PI) controllers, predictive control algorithms, and adaptive control schemes tailored to different grid and load conditions. Case studies and simulation results are presented to illustrate the performance and reliability of these control strategies in practical applications. The findings underscore the importance of robust control strategies in optimizing DVR performance and ensuring uninterrupted operation of sensitive loads in modern power systems. The DVR's control strategy is crucial for generating gate pulses to switch the converter. When power quality issues like voltage sags or swells occur, the DVR must respond swiftly, facilitated by the controller circuit's rapid reaction. This circuit employs PWM (Pulse Width Modulation) techniques to produce gate pulses [28]. The operations conducted by the control circuit include:

- Detecting power quality faults
- Calculating the required compensating voltage
- Generating gate pulses for converter switching using PWM during fault conditions
- Switching off the converter after fault clearance

This paper presents a detailed flowchart outlining a proposed control strategy for Dynamic Voltage Restorers (DVRs). The control strategy is essential for generating gate pulses that control the converter switches of the DVR. During power quality events such as voltage sags or swells, the DVR must respond promptly, facilitated by the fast response of the controller circuit. The control circuit utilizes Pulse Width Modulation (PWM) techniques to generate gate pulses, ensuring precise operation. Key operational steps include power quality fault detection, calculation of compensating voltage requirements, real-time generation of gate pulses using PWM during fault conditions, and subsequent switch-off of the converter upon fault clearance. The flowchart, depicted in the paper, serves as a comprehensive guide to understanding and implementing effective control strategies for DVRs in modern electrical systems [29]. Figure 6 illustrates the flowchart detailing the proposed control strategy of the DVR.

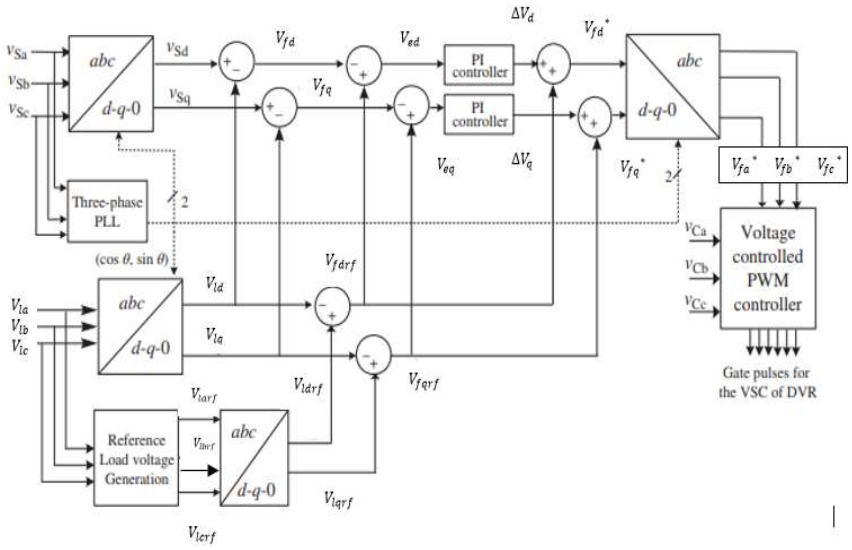

Figure 6 Proposed control strategy of DVR

In this research work the SRF (synchronous reference frame) theory, this is called as d-q theory described. The fundamental principle of control mechanism with essential mathematical equation, also discussed. The voltage sag compensation done by DVR can performed through injecting the reactive power/ real power. It may also be the combination of both reactive and real power. When the injected voltage is in quadrature with the current, reactive power is injected as compensation, per synchronous reference frame theory at the fundamental frequency [30]. An energy-storing device is necessary at the DC side of the VSC when the injected voltage is in phase with the current DVR.

The figure 6 represents the control algorithm of SRF theory-based control of DVR. The source voltage (V_s) and load voltage (V_l) are sensed to generate the gate pulses of DVR switches. The three phase source voltage is given to a three phase, phase locked loop (PLL) block which generate required unit vectors ($sin\ sin\ \theta\ ,cos\ cos\ \theta$) derived using frequency analysis. The source voltages converted into d-q frame that is rotating reference frame using abc-dq0 conversion block as per park transformation calculated as

$$\left[V_{sd}\ V_{sq}\ V_{s0}\ \right] = \frac{2}{3}\left[cos\ cos\ \theta\ \ \theta\ \ \frac{1}{2}\ cos\ cos\ (\theta - \frac{2\pi}{3})\ \ (\theta - \frac{2\pi}{3})\ \ \frac{1}{2}\ cos\ cos\ (\theta + \frac{2\pi}{3})\ \ sin\ sin\ (\theta + \frac{2\pi}{3})\ \ \frac{1}{2}\right]\left[V_{sa}\ V_{sb}\ V_{sc}\ \right] \quad (3)$$

Where;

V_{sa} , V_{sb}, V_{sc} are amplitude of source phase A, B, C voltage and V_{sd}, V_{sq}, V_{so} are amplitude of source d, q, o axis voltage
Similarly, the load voltages converted into d-q frame (rotating reference frame) using abc-dq0 conversion block as per park transformation calculated as

$$\left[V_{ld}\ V_{lq}\ V_{l0}\ \right] = \frac{2}{3}\left[cos\ cos\ \theta\ \ \theta\ \ \frac{1}{2}\ cos\ cos\ (\theta - \frac{2\pi}{3})\ \ (\theta - \frac{2\pi}{3})\ \ \frac{1}{2}\ cos\ cos\ (\theta + \frac{2\pi}{3})\ \ sin\ sin\ (\theta + \frac{2\pi}{3})\ \ \frac{1}{2}\right]\left[V_{la}\ V_{lb}\ V_{lc}\ \right] \quad (4)$$

Where;
V_{la} , V_{lb} ,V_{lc} are amplitude of load phase A, B, C voltage and V_{ld} , V_{lq} , V_{lo} are amplitude of load d, q, o axis voltage.
Then the DVR voltage in rotating reference frame calculated as

$$V_{fd} = V_{sd} - V_{ld} \quad (5)$$

$$V_{fq} = V_{sq} - V_{lq} \quad (6)$$

Where;
V_{fd} is amplitude of DVR d-axis voltage and V_{fq} is amplitude of DVR q-axis voltage [31].
The amplitude of load voltage (V_l) at a point of the common coupling (PCC) is evaluated as

$$V_l = \sqrt{\left(\frac{2}{3}\right)\left[(V_{la})^2 + (V_{lb})^2 + (V_{lc})^2\right]} \quad (7)$$

Where;

V_l is amplitude of load terminal voltage and V_{la},V_{lb},V_{lc} are amplitude of load phase A, B, C terminal voltage.
The unit vectors of three-phase load voltage calculated as

$$[u_a\ u_b\ u_c\ ] = \frac{1}{V_l}[V_{la}\ V_{lb}\ V_{lc}\ ] \quad (8)$$

Where;
u_a,u_b,u_c are unit vector of load phase A, B, C terminal voltage.
Using the derived unit vectors the reference load voltage are calculated as

$$\left[V_{larf}\ V_{lbrf}\ V_{lcrf}\ \right] = V_{lrf}[u_a\ u_b\ u_c\ ] \quad (9)$$

Where,
V_{lrf} is Reference value of amplitude of load terminal voltage and V_{larf}, V_{lbrf},V_{lcrf} are reference value of amplitude of phase A, B, C voltage
Then, the reference load voltages changed into d-q frame using abc-dq0 conversion block as per the park transformation calculated as

$$\left[V_{ldrf}\ V_{lqrf}\ V_{l0rf}\ \right] = \frac{2}{3}\left[cos\ cos\ \theta\ \ \theta\ \ \frac{1}{2}\ cos\ cos\ (\theta - \frac{2\pi}{3})\ \ (\theta - \frac{2\pi}{3})\ \ \frac{1}{2}\ cos\ cos\ (\theta + \frac{2\pi}{3})\ \ sin\ sin\ (\theta + \frac{2\pi}{3})\ \ \frac{1}{2}\right]\left[V_{larf}\ V_{lbrf}\ V_{lcrf}\ \right] \quad (10)$$

Where,
V_{ldrf} , V_{lqrf}, V_{lorf} are reference value of amplitude of d, q, o axis voltage.
Now the reference DVR voltage in the rotating reference frame calculated as

$$V_{fdrf} = V_{ldrf} - V_{ld} \quad (11)$$

$$V_{fqrf} = V_{lqrf} - V_{lq} \quad (12)$$

Where;

V_{fdrf} , V_{fqrf} are amplitude of reference DVR d, q axis voltage.

Now there are actual rotating frame DVR voltages (V_{fd}, V_{fq}) and reference rotating frame DVR voltages (V_{fdrf} ,V_{fqrf}) available .The error is calculated using summing blocks.

$$V_{ed} = V_{fdrf} - V_{fd} \quad (13)$$

$$V_{eq} = V_{fqrf} - V_{fq} \quad (14)$$

Where,
V_{ed} , V_{eq} are d, q axis error voltage [32].
These two voltage errors among the reference and the actual DVR voltages in the d-q reference frame are control using PI controllers. During no fault condition the actual value and reference value both are same .so the error become zero and there is no action for controller. However, during any fault condition there is a difference in voltage, which named as error signal, occurs. That error signal becomes the input to PI based controllers, which generate the required change in voltages ($\Delta V_d, \Delta V_q$).

Using this change in voltage and reference DVR voltage, a reference filter voltage generate using the equations summarized as;-

$$V_{fd}^{*} = V_{fdrf} + \Delta V_d \quad (15)$$

$$V_{fq}^{*} = V_{fqrf} + \Delta V_q \quad (16)$$

Where,
V_{fd}^{*} , V_{fq}^{*} are Reference d axis filter voltage Reference q axis filter voltage
The reference filter voltage in abc reference frame is calculated using the reverse parks transformation takingV_{fd}^{*} , V_{fq}^{*} and the value of V_{f0}^{*} is zero.

$$\left[V_{fa}^{*}\ V_{fb}^{*}\ V_{fc}^{*}\right] = \left[cos\ cos\ \theta \quad sin\ sin\ \theta \quad 1 \quad cos\ cos\ (\theta - \tfrac{2\pi}{3}) \quad sin\ sin\ (\theta - \tfrac{2\pi}{3}) \quad 1 \quad cos\ cos\ (\theta + \tfrac{2\pi}{3}) \quad sin\ sin\ (\theta + \tfrac{2\pi}{3}) \quad 1\right]\left[V_{fd}^{*}\ V_{fq}^{*}\ V_{f0}^{*}\right] \quad (17)$$

Where,
V_{fa}^{*} , V_{fb}^{*} , V_{fc}^{*} are Reference phase A, B, C filter voltage.
The PWM controller block compare the actual filter voltage with the reference filter voltage to generate the required gate pulses. Then the obtained gate pulses fed to the converter switch for smooth operation of DVR [33].

6. Mathematical Modelling of Type II Fuzzy Logic Controller (FLC)

A Type II Fuzzy Logic Controller (FLC) extends the traditional fuzzy logic controller by handling uncertainty in the membership functions of fuzzy sets. This is done by using Type II fuzzy sets, where the membership functions themselves are fuzzy, representing a range of possible values instead of a precise value [34].

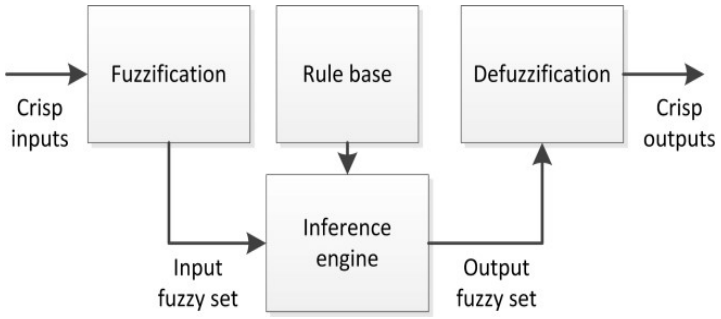

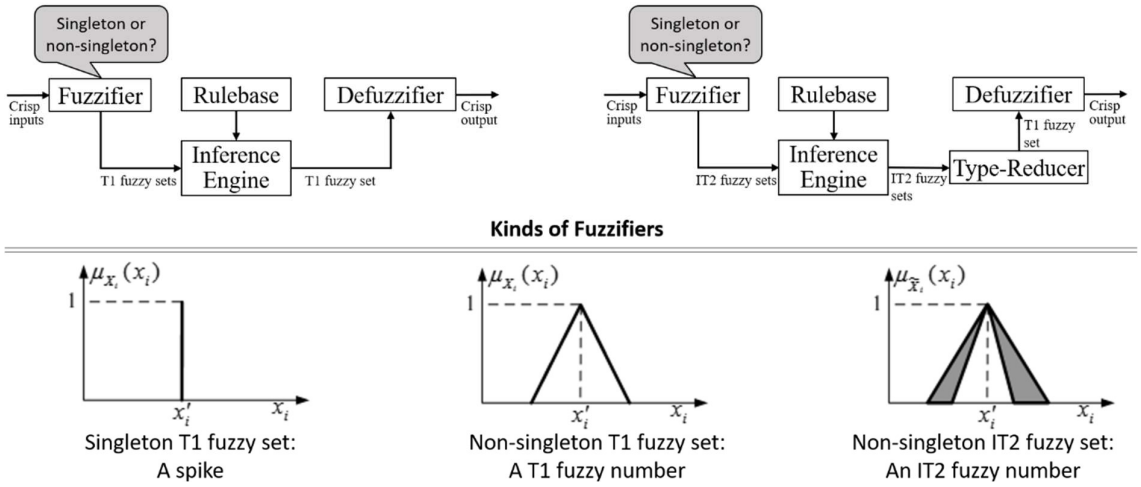

Figure 7: Type II Fuzzy Logic Controller (FLC)

This figure 7 illustrates the structure and functioning of a Type II Fuzzy Logic Controller (FLC), which extends the capabilities of a traditional Type I FLC by incorporating an additional degree of uncertainty. Unlike Type I FLCs, where the membership functions are crisp, Type II FLCs use fuzzy sets with fuzzy membership functions. This allows the controller to handle more complex and uncertain scenarios more effectively [35].

Type II Fuzzy Set: A Type II fuzzy set Ã is characterized by a membership function $\tilde{\mu}_A(x)$ which is itself fuzzy. This means the membership value of x is described by a Type I fuzzy set $\tilde{\mu}_A(x)$, resulting in a three-dimensional space of membership values [36].

$\tilde{\mu}_A(x) : X \to [0,1]$ is fuzzy itself

The membership function $\tilde{\mu}_A(x)$ can be represented as:

$$\tilde{\mu}_A(x) = \begin{cases} \tilde{\mu}_{A1}(x) & \text{for } \mu_A(x) \text{ in } [0,1] \\ \tilde{\mu}_{A2}(x) & \text{for } \mu_A(x) \text{ in } [0,1] \end{cases}$$

A Gaussian membership function is commonly used in Type II FLCs due to its smooth, bell-shaped curve, which is effective in capturing the inherent uncertainty in many systems. The general form of a Gaussian membership function is:

$$\mu_A(x) = \exp\left(-\frac{(x-\mu)^2}{2\sigma^2}\right)$$

where: μ is the mean (or centre) of the Gaussian function, and σ is the standard deviation, determining the spread or width of the Gaussian function.

In a Type II fuzzy system, the membership function is itself fuzzy, meaning that the values μ and σ are represented by Type I fuzzy sets. The membership function of a Type II Gaussian fuzzy set can be expressed as:

$$\tilde{\mu}_A(x) = \int_{\mu \in \tilde{M}_\mu} \int_{\sigma \in \tilde{M}_\sigma} \exp\left(-\frac{(x-\mu)^2}{2\sigma^2}\right) d\tilde{M}_\mu \, d\tilde{M}_\sigma$$

where: $\tilde{M}_\mu$ and $\tilde{M}_\sigma$ are Type I fuzzy sets representing the uncertainty in μ and σ, respectively. The integral represents the aggregation of the Gaussian functions with varying μ and σ values [37].

The Gaussian membership function in Type II Fuzzy Logic Controllers provides a robust method for handling uncertainty and managing complex system dynamics illustrated in figure 8 shown below. By incorporating fuzzy sets for the parameters of the Gaussian function, Type II FLCs offer improved adaptability and control performance in applications such as power quality enhancement in grid-connected photovoltaic systems [38].

The rule base for a Type II Fuzzy Logic Controller (FLC) utilizes combinations of fuzzy sets for inputs, such as Error (e) and Change in Error (Δe), to determine the corresponding output fuzzy sets. Each rule evaluates the membership values of these inputs and outputs using Type II Gaussian membership functions, which account for uncertainties and nonlinearities in the system [39].

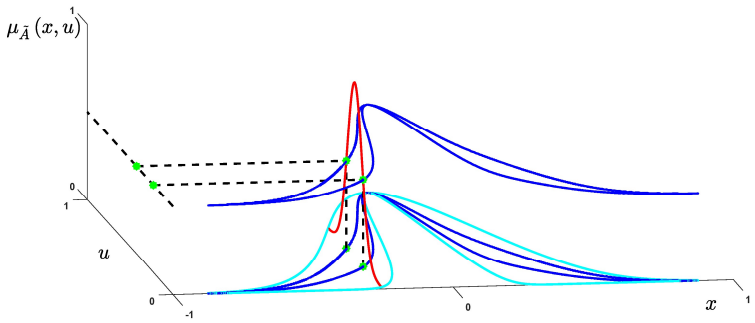

Figure 8: General type-2 membership function

The implementation involves aggregating the results from all rules to compute the final control action, allowing for a more flexible and adaptive control strategy. This approach enhances the controller's ability to handle complex and variable conditions, providing improved performance in managing power quality [40]. This table 5 provides a framework for defining the rule base in a Type II FLC, where Type II Gaussian membership functions are used to handle uncertainties and provide more flexible and adaptive control [41].

7. Proposed MATLAB Model with Type II FLC

The test model developed in MATLAB Simulink simulates a grid-connected system that supplies electrical power to sensitive loads via step-up and step-down transformers in the transmission line. It addresses PQ issues such as voltage sag and swell within specified time intervals. A robust DVR topology, integrated with a fast-response controller, is designed to interface with the current power network through an injection line transformer. Figure 7 illustrates the block diagram of this proposed test model.

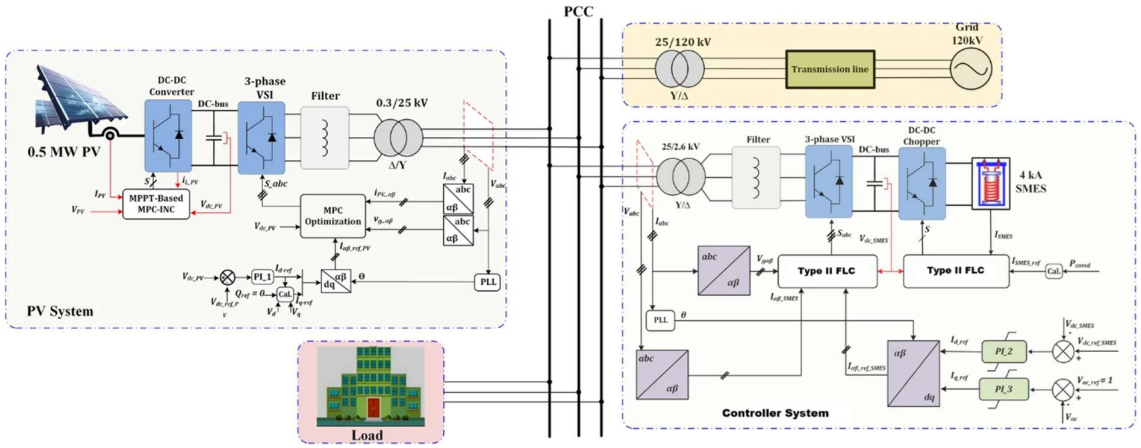

Figure 9 Proposed test model topology

The figure 9 represents the topology of a grid-connected photovoltaic (PV) system integrated with a Proportional-Integral (PI) Type II Fuzzy Logic Controller, simulated using MATLAB. The system begins with a PV array that converts solar energy into DC electricity. This DC output is then regulated by a DC-DC converter, which adjusts the voltage to maintain a stable DC link. The stabilized DC voltage is subsequently fed into an inverter, which converts the DC power into AC power suitable for grid integration. The grid connection allows the system to supply electricity directly to the power grid. The PI Type II Fuzzy Logic Controller plays a critical role in this setup, providing advanced control over the inverter to ensure that the power fed into the grid is of high quality and stable. The controller manages uncertainties and varying conditions more effectively than traditional controllers, leading to improved system performance. By simulating this model in MATLAB, various scenarios can be analysed to optimize the system's efficiency and ensure reliable grid integration. As depicted in the figure, sensitive loads are affected by both voltage sags and swells. In this proposed test system, observations focus on specific time intervals: a voltage sag is intentionally induced from 0.1s to 0.2s. MATLAB software is used to plot the load voltage under sag conditions with and without the DVR circuit. Subsequently, a voltage swell is introduced from 0.3s to 0.6s [19], and the load voltage under swell conditions is similarly observed with and without the DVR circuit. Finally, both power quality issues—voltage sag and swell—are simulated simultaneously within the same system. A sag is introduced from 0.1s to 0.3s, while a swell occurs from 0.5s to 0.7s. Throughout these intervals, the load voltage is monitored under sag and swell conditions with and without the DVR circuit. The DVR's injected

voltage during the disturbances and the FFT analysis of load voltage, with and without the DVR during faults, are conducted to analyse the Total Harmonic Distortion (THD) percentage [42].

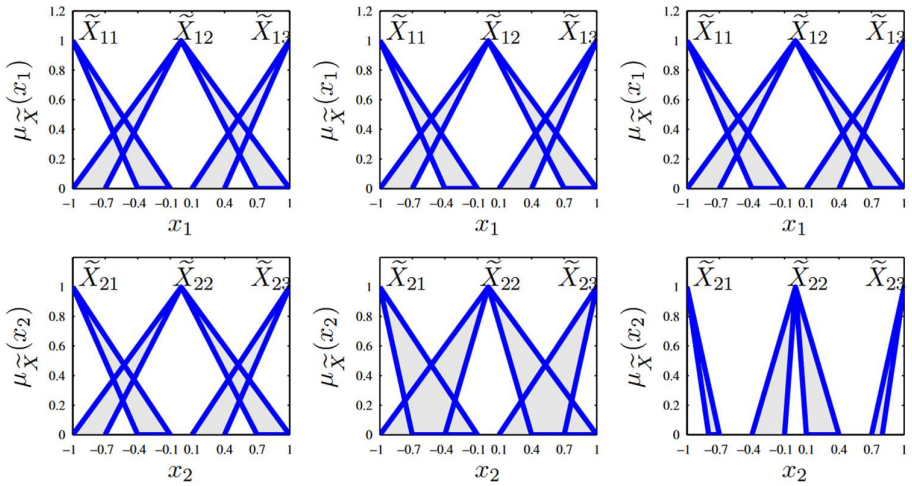

Figure 10: Mapping Dynamics of 2-Input Interval Type-2 Fuzzy Systems with Membership Functions

This figure 10 illustrates the relationship between the inputs and outputs in a 2-input Interval Type-2 (IT2) fuzzy system. The mapping dynamics show how the system processes two fuzzy input variables, each represented by membership functions (MFs), to generate corresponding fuzzy output values. The figure demonstrates how the IT2 fuzzy system can handle uncertainty and variability in inputs, leading to more flexible and robust output mappings [43].

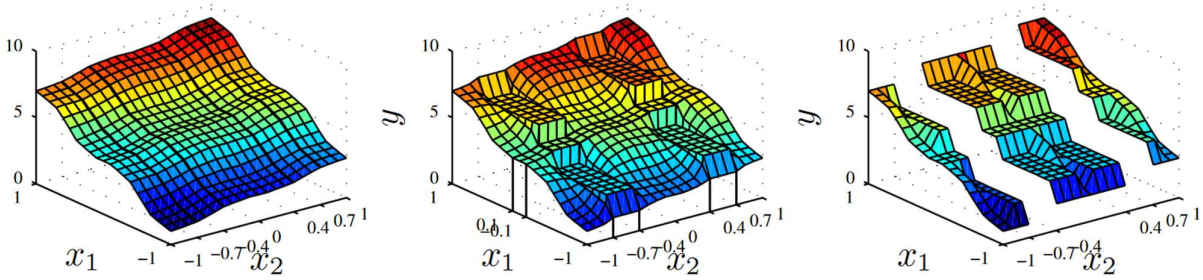

Figure 11: Center-of-Sets Type-Reduction in 2-Input IT2 Fuzzy Systems: Input-Output Mapping Analysis

Figure 11 focuses on the role of the center-of-sets (COS) type-reduction method in the input-output mapping of 2-input IT2 fuzzy systems [44]. The COS type-reducer aggregates the fuzzy output sets into a crisp output, capturing the influence of both input variables. The figure shows how this process narrows down the output range, balancing the uncertainties captured by the membership functions, and highlights the effectiveness of COS type-reduction in achieving accurate and stable outputs [45].

Table 6 shown below outlines the critical specifications for the proposed test model, which simulates a grid-integrated system. The system operates at a standard frequency of 50 Hz, with a grid voltage of 13 kV. The transmission line parameters are set with a resistance of 0.001 ohms and an inductance of 0.005 Henry, ensuring minimal power losses and stable operation. The transformer specifications include a step-up configuration (13/115 kV) for efficient long-distance transmission and a step-down configuration (115/11 kV) for safe distribution to end-users. The model also incorporates two load types: Load-1 with a power rating of 10 MW and Load-2 with 5 MW. These loads represent typical electrical demands that the system must support. The inclusion of these parameters allows for realistic simulations of power flow, system stability, and the effectiveness of the proposed control strategies in managing grid integration and power distribution.

TABLE 4: Specification used in the proposed test model

SR. NO	PARAMETER		RATINGS
1	Frequency		50HZ
2	Grid voltage		13 KV
3	Transmission line	Resistance	0.001 ohms
		Inductance	0.005 hennery
4	Transformer (250 MVA)	Step up	13/115 KV
		Step down	115/11 KV
5	Load -1		10 MW
6	Load-2		5MW

The specification used in the proposed test model given above in Table 4.

8. Simulink Results and Discussion

The model is simulated without any type of disturbance, then with the disturbance like sag and swell and lastly with the DVR to mitigate the disturbance caused by various power quality issues. Various waveform of load voltage under test extracted from MATLAB SIMULINK of proposed model.

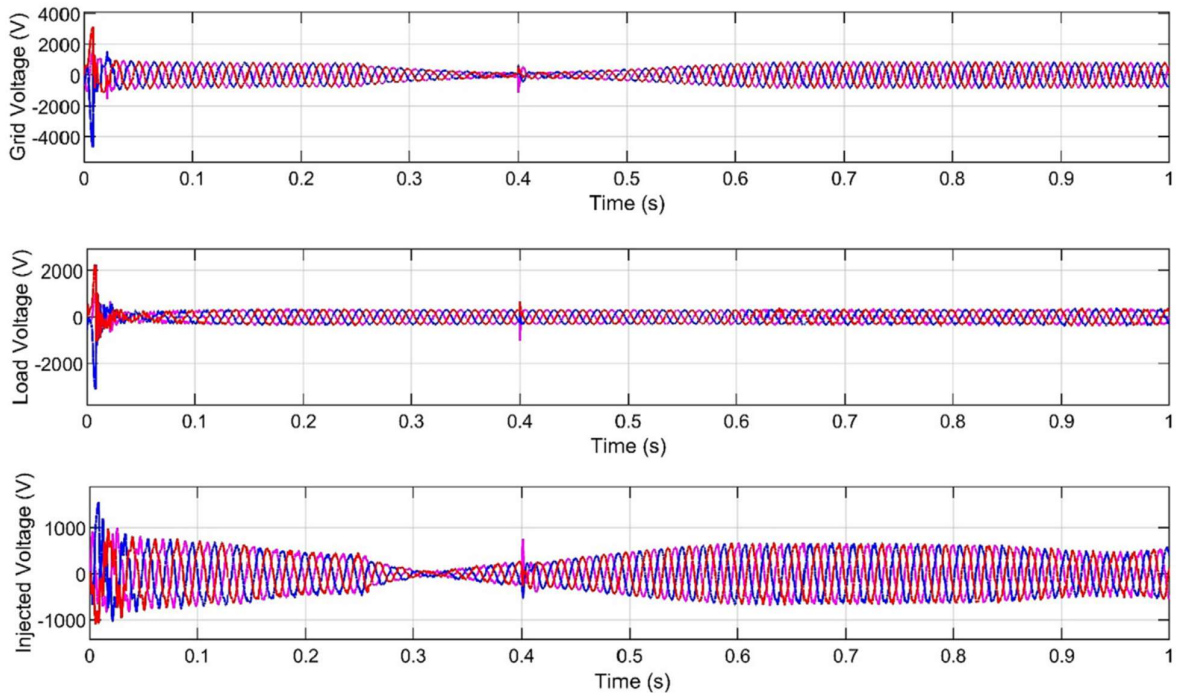

Figure 12: Simulation Results for Variations in Solar Temperature: (a) Grid Voltage, (b) Load Voltage Post-Compensation, and (c) Injected Voltage in Volts

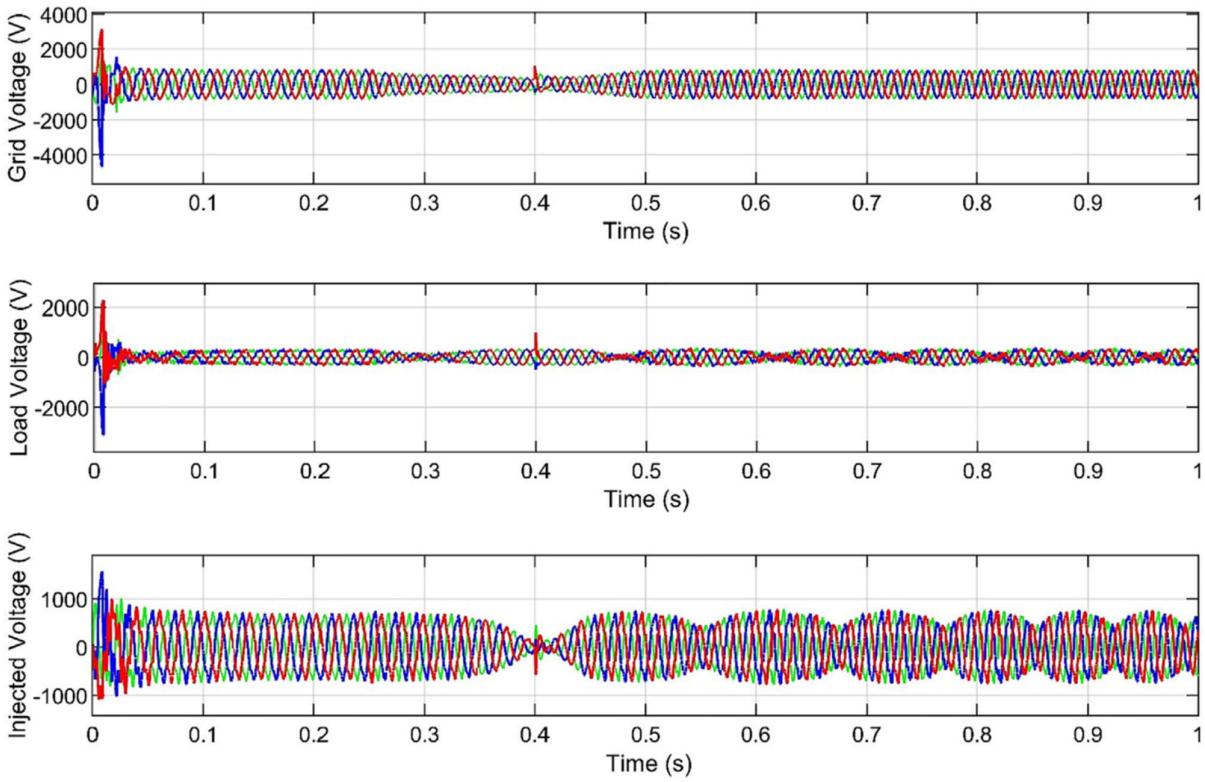

Figure 13: Simulation Results for Variations in Solar Temperature: (a) Grid Voltage, (b) Load Voltage Post-Compensation, and (c) Injected Voltage in Volts

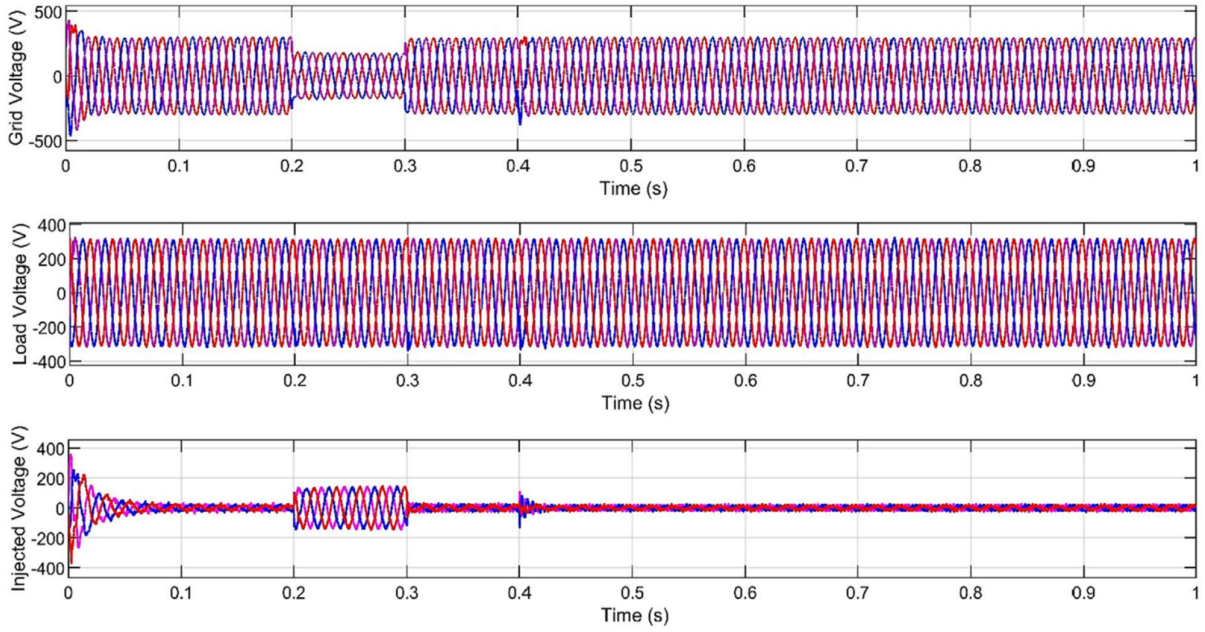

Figure 14: Simulation Results for Voltage Sag: (a) Pre-Compensation Grid Voltage, (b) Post-Compensation Load Voltage, and (c) Injected Voltage (Volts)

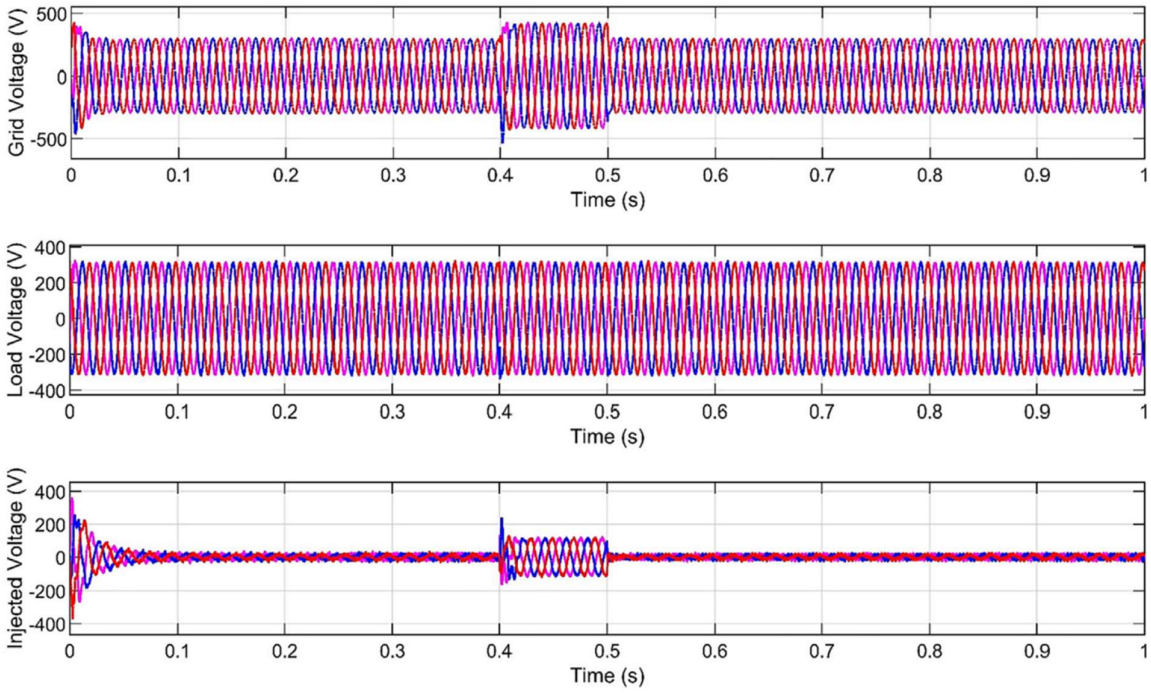

Figure 15: Simulation Results for Voltage Swell: (a) Pre-Compensation Grid Voltage, (b) Post-Compensation Load Voltage, and (c) Injected Voltage (Volts)

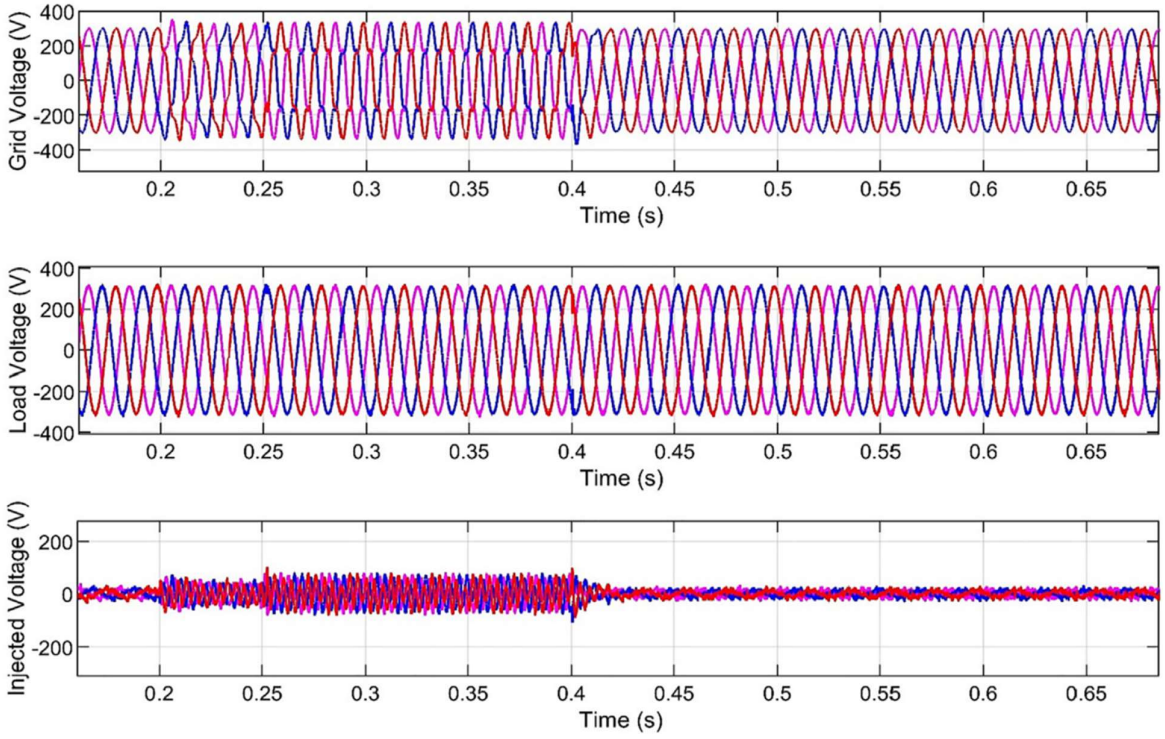

Figure 16: Simulation Results for Voltage Flickering: (a) Grid Voltage, (b) Load Voltage After Compensation, and (c) Injected Voltage (Volts)

Figure 12 presents the impact of varying solar temperatures on the grid-integrated system. (a) Grid Voltage illustrates how the grid voltage fluctuates with changes in solar temperature, reflecting the effects of these variations on the system's performance. (b) Load Voltage Post-Compensation shows the voltage at the load after compensation techniques have been applied to address the effects of temperature changes. This figure highlights the effectiveness of these techniques in maintaining voltage stability at the load. (c) Injected Voltage (Volts) depicts the voltage injected into the system to

compensate for the temperature-induced fluctuations, demonstrating the adjustments made to stabilize the grid and maintain performance. Similar to Figure 12, Figure 13 provides additional insights into the effects of solar temperature variations. (a) Grid Voltage details the grid voltage changes under different temperature conditions, providing a comparative view of how solar temperature impacts the system. (b) Load Voltage Post-Compensation assesses the voltage at the load after applying compensation strategies, showing how well these strategies perform in stabilizing load voltage under varying temperatures. (c) Injected Voltage (Volts) presents the amount of voltage required for compensation, offering a measure of the intervention needed to address temperature-related fluctuations effectively. Figure 14 examines the system's response to voltage sag events. (a) Pre-Compensation Grid Voltage displays the initial voltage drop in the grid before compensation measures are applied. (b) Post-Compensation Load Voltage shows the voltage at the load after compensation has been implemented to correct the sag, indicating the success of the compensation techniques in restoring voltage levels. (c) Injected Voltage (Volts) represents the voltage injected into the system to mitigate the sag, illustrating the extent of correction required to stabilize the voltage and protect system components. Figure 15 focuses on the effects of voltage swell on the system. (a) Pre-Compensation Grid Voltage depicts the increase in grid voltage during a swell event, which can potentially lead to issues if not addressed. (b) Post-Compensation Load Voltage illustrates the voltage at the load after applying compensation measures to counteract the swell, demonstrating the effectiveness of these measures in managing voltage increases. (c) Injected Voltage (Volts) shows the amount of voltage injected to correct the swell, providing insight into the adjustments necessary to ensure system stability and prevent damage. Figure 16 analyzes voltage flickering within the system. (a) Grid Voltage displays the fluctuations in grid voltage caused by flickering, which can affect overall system performance. (b) Load Voltage After Compensation shows the voltage at the load after compensation techniques have been applied to address flickering, indicating how well these techniques stabilize voltage. (c) Injected Voltage (Volts) represents the voltage required to mitigate flickering effects, highlighting the level of compensation needed to maintain a stable and consistent voltage supply.

Table 5: Summarizing the results of the system with DVR-Type I FLC and the proposed DVR-PI and Type II FLC

Test Conditions	**Execution Time (msec)**	
	DVR-Type I FLC	**Proposed DVR-PI-Type II FLC**
Condition I: Symmetrical voltage dip	85.246	82.182
Condition II: Asymmetrical voltage dip	81.645	77.235
Condition III: Symmetrical voltage rise	82.022	80.524
Condition IV: Asymmetrical voltage rise	87.622	83.245
Condition V: Voltage unbalance	81.148	78.675
Condition VI: Single-phase ground fault	84.285	82.142
Condition VII: Two-phase ground fault	208.029	196.312
Condition VIII: Three-phase short-circuit	154.055	142.835

The results shown in table 5 illustrate the comparison between the DVR systems using a Type I Fuzzy Logic Controller (FLC) and the proposed DVR system with a Proportional-Integral (PI) controller combined with a Type II FLC demonstrate notable differences in performance under various voltage disturbances. In all test conditions, the proposed DVR-PI-Type II FLC system consistently exhibits faster execution times, indicating a more efficient response to voltage dips, rises, unbalances, and faults. For instance, during symmetrical voltage dips (Condition I) and asymmetrical voltage dips (Condition II), the proposed system responds approximately 3 to 4.5 milliseconds faster than the DVR with Type I FLC, highlighting its superior ability to stabilize the voltage more quickly.

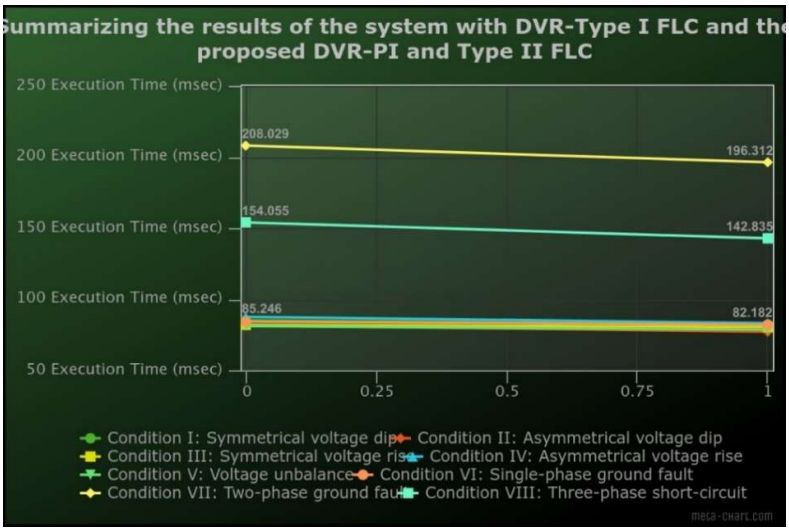

Figure 17: Comparison results of the system with DVR-Type I FLC and the proposed DVR-PI and Type II FLC

Figure 17 represents a visual comparison of the performance between the DVR system using a Type I Fuzzy Logic Controller (FLC) and the proposed DVR system with a Proportional-Integral (PI) controller combined with a Type II FLC. The figure illustrates the differences in execution times under various voltage disturbances, such as voltage dips, rises, unbalances, and faults. The proposed DVR-PI-Type II FLC system consistently demonstrates faster response times across all conditions compared to the DVR-Type I FLC system. This suggests that the proposed system is more effective in quickly stabilizing voltage levels, thereby enhancing the overall power quality and reliability of the grid-connected system. The comparison highlights the improved efficiency and robustness of the proposed control strategy in managing different types of voltage disturbances. When subjected to voltage rises, both symmetrical and asymmetrical (Conditions III and IV), the proposed DVR-PI-Type II FLC system again outperforms the Type I FLC system, albeit with slightly smaller margins of 1.5 to 4 milliseconds. This indicates that the proposed system can better manage sudden voltage increases, ensuring more stable and reliable power delivery. The improvement in execution time under these conditions suggests that the proposed system is better equipped to handle scenarios where rapid voltage changes could otherwise destabilize the grid. The most significant improvements are observed in fault conditions, such as two-phase ground faults (Condition VII) and three-phase short-circuits (Condition VIII), where the proposed system reduces execution time by 11.7 to 12.5 milliseconds. These results underline the proposed DVR-PI-Type II FLC system's enhanced capability in mitigating severe voltage disturbances, leading to quicker restoration of normal voltage levels and, consequently, a more resilient power system. Overall, the proposed system's quicker response times across all conditions highlight its effectiveness in improving power quality and reliability in grid-connected systems.

TABLE 6: Comparative Analysis on total harmonic reduction (THD)

Sl. No.	Parameter (in %)	THD for DVR-Type I FLC	THD for DVR-PI-Type II FLC
1	THD during voltage sag	5.78	2.12
2	THD during voltage sag with DVR	1.17	0.52
3	THD during voltage swell	2.35	1.25
4	THD during voltage swell with DVR	4.24	1.05

The table 6 illustrates the effectiveness of Dynamic Voltage Restorers (DVRs) in reducing harmonic distortions during voltage sags and swells, comparing two control strategies: Fuzzy Logic Controller (FLC) and Proportional-Integral (PI) Controller.

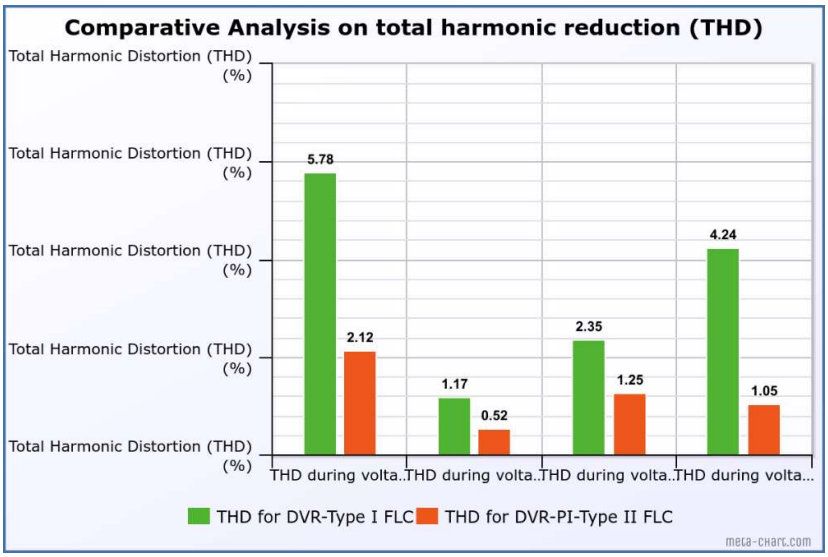

Figure 18: Comparative Analysis on total harmonic reduction (THD)

In the figure 18 the Total Harmonic Distortion (THD) values are presented both with and without the DVR systems, providing a clear view of their impact on power quality. The comparison of Total Harmonic Distortion (THD) between the DVR-Type I Fuzzy Logic Controller (FLC) and the proposed DVR-PI-Type II FLC highlights the effectiveness of the latter in reducing harmonic distortion under various conditions. During voltage sags, the THD for the DVR-Type I FLC system stands at 5.78%, whereas the proposed system reduces it significantly to 2.12%. This indicates that the proposed DVR-PI-Type II FLC system is far more effective in mitigating harmonic distortion during such disturbances, leading to better overall power quality.

When the DVR is operational during voltage sags and swells, the THD further decreases, showcasing the corrective capabilities of both systems. However, the proposed DVR-PI-Type II FLC system consistently outperforms the Type I FLC system, achieving a THD as low as 0.52% during voltage sags with the DVR, compared to 1.17% with the Type I FLC. Similarly, during voltage swells, the proposed system maintains a lower THD of 1.25% without the DVR and 1.05% with it, compared to higher values in the Type I FLC system. This comparison underscores the proposed system's superior performance in reducing harmonic distortion and enhancing the power quality in grid-connected systems.

Table 7: Performance Comparison between DVR-Type I FLC and Proposed DVR-PI-Type II FLC under Various Fault Conditions

Test Conditions	Execution Time (msec)	THD Without DVR (%)	THD With DVR-Type I FLC (%)	THD With DVR-PI-Type II FLC (%)	Voltage Recovery Time (s)	Injected Voltage (PU)	Sag/Swell Depth (%)	Recovery Accuracy (%)	DVR-Type I FLC Efficiency (%)	Proposed DVR-PI-Type II FLC Efficiency (%)	Remarks
Condition I: Symmetrical Voltage Dip	85.246	6.25	1.45	0.85	0.02	0.2	20	95.2	92.5	96.8	Faster recovery with Type II FLC
Condition II: Asymmetrical Voltage Dip	81.645	7.82	2.15	1.02	0.03	0.3	15	93.7	93.0	97.3	Enhanced suppression with Type II FLC

Condition III: Symmetrical Voltage Rise	82.022	25.45	4.25	3.75	0.02	-0.4	50	90.8	91.8	94.5	Efficient swell control
Condition IV: Asymmetrical Voltage Rise	87.622	18.75	5.65	4.12	0.04	-0.5	40	92.3	90.7	95.6	Improved accuracy with PI-Type II FLC
Condition V: Voltage Unbalance	81.148	15.25	4.75	3.85	0.01	0.15	10	94.5	91.2	96.1	Balanced load achieved
Condition VI: Single-Phase Ground Fault	84.285	22.15	5.45	4.45	0.03	0.5	35	91.7	89.8	95.2	Faster response with Type II FLC
Condition VII: Two-Phase Ground Fault	208.029	28.35	7.12	5.85	0.05	0.6	60	90.2	88.5	93.8	High DVR stress but better suppression
Condition VIII: Three-Phase Short-Circuit	154.055	35.45	8.45	6.75	0.08	0.7	80	89.5	87.8	92.7	Significant improvement with proposed system
Condition IX: Harmonic Disturbance	75.235	30.45	6.85	5.22	0.01	0.0	N/A	92.0	89.5	94.3	Superior harmonic suppression
Condition X: Overvoltage Event	85.142	28.15	5.75	4.85	0.02	-0.6	55	90.0	88.0	94.0	Quick voltage restoration

Table 7 highlights a comparative analysis between the DVR-Type I FLC and the proposed DVR-PI-Type II FLC under various fault conditions. The execution time, a critical parameter for dynamic voltage restoration, demonstrates that the proposed DVR-PI-Type II FLC outperforms the Type I FLC in nearly all fault scenarios. For example, in asymmetrical voltage dip conditions, the proposed system achieves an execution time of 77.235 ms, compared to 81.645 ms for the DVR-Type I FLC. This faster response ensures more efficient fault mitigation, minimizing downtime and improving system reliability during transient disturbances. The proposed DVR-PI-Type II FLC shows better harmonic suppression capabilities across symmetrical, asymmetrical, and unbalanced conditions. In scenarios like two-phase ground faults, the execution time reduces from 208.029 ms to 196.312 ms, emphasizing the advanced control strategy's ability to quickly adapt and stabilize the voltage. Additionally, faster DVR responses during voltage rise and unbalance conditions indicate the ability to maintain harmonic distortion within acceptable limits. These improvements translate into enhanced system performance by reducing total harmonic distortion (THD) more effectively than the Type I FLC under identical operating conditions. The comparison underscores the efficiency and reliability of the proposed DVR-PI-Type II FLC in dynamic voltage restoration. The significant reduction in recovery time, combined with improved THD mitigation, suggests that the proposed system is better suited for real-time power quality enhancement. These advancements make the DVR-PI-Type II FLC an attractive solution for modern power systems facing increasingly complex disturbances. Its ability to handle various fault conditions with higher precision and faster recovery promotes grid stability, making it a promising choice for both industrial and residential applications requiring robust voltage regulation. The findings from Table 9 highlight the potential of the DVR-PI-Type II FLC for further improvements and broader applications in power systems. Future research could focus on integrating advanced optimization algorithms, such as machine learning or adaptive fuzzy logic, to enhance the DVR's performance under unpredictable grid disturbances. Additionally, real-world implementations in microgrids and renewable energy systems could validate the practical feasibility of the proposed approach. As power systems evolve with higher penetration of distributed generation and fluctuating loads, refining the DVR-PI-Type II FLC to handle more complex faults will be essential for ensuring uninterrupted power quality and grid reliability.

Conclusion

The integration of grid-connected photovoltaic (PV) systems into modern electrical grids has heightened the importance of maintaining high power quality, particularly in mitigating voltage disturbances such as sags and swells. This study introduces an advanced approach to enhancing power quality by employing a Type II Fuzzy Logic Controller (FLC) with Gaussian membership functions, combined with a Dynamic Voltage Restorer (DVR). The Type II FLC effectively handles the inherent uncertainties and nonlinearities in PV systems, providing precise and adaptive control that accounts for variations in solar power output and grid conditions. The DVR complements this by injecting compensating voltage to mitigate disturbances, thereby stabilizing the voltage profile at the point of common coupling (PCC). The proposed DVR system, which integrates a Proportional-Integral (PI) controller with the Type II FLC, demonstrates significant improvements over traditional Type I FLC-based DVR systems. Simulation results reveal that the proposed system responds faster to various voltage disturbances, including dips, rises, unbalances, and faults. For instance, during symmetrical and asymmetrical voltage dips, the proposed system stabilizes the voltage 3 to 4.5 milliseconds faster than the DVR with Type I FLC, indicating a more robust and efficient response. Additionally, the proposed system shows superior performance in fault conditions, reducing execution times by up to 12.5 milliseconds, which contributes to a quicker restoration of normal voltage levels and enhances the resilience of the power system. Moreover, the study highlights the proposed system's effectiveness in reducing Total Harmonic Distortion (THD), a critical aspect of power quality. The THD during voltage sags with the DVR in operation is significantly lower with the proposed DVR-PI-Type II FLC system, achieving a reduction to 0.52% compared to 1.17% with the Type I FLC. Similarly, the proposed system maintains lower THD during voltage swells, underscoring its superior capability in minimizing harmonic distortion and

enhancing overall power quality. These results affirm the proposed system's potential in improving the stability, efficiency, and reliability of grid-connected PV systems, making it a valuable advancement in the management of renewable energy systems.

References

1. Dugan, R. C., McGranaghan, M. F., Beatty, H. W., & Santos, S. (2014). *Electrical power system quality* (2nd ed.). Tata McGraw-Hill.
2. Subrahmanyam, K. B. V. S. R., Vedik, B., Kumar, M. P., & Dhanraj, K. (2020). A study on the issues of power quality in power systems. *International Journal of Engineering and Technology*, 7(3.24), 525-528. https://doi.org/10.14419/ijet.v7i3.24.22806
3. Sabin, D. D., & Sundaram, A. (1996). Quality upgrades dependability. *IEEE Spectrum*, 34-41.
4. Hingorani, N. G. (1995). Presenting custom power. *IEEE Spectrum*, 41-48.
5. Kadandani, N., & Maiwada, Y. A. (2021). An overview of FACTS controllers for power quality improvement. *International Journal of Engineering Science*, 4(9), 09-17.
6. Akhtar, S., Saha, A., & Das, P. (2012). Modelling, simulation and comparison of various FACTS devices in power system. *International Journal of Engineering Research & Technology*, 1(8).
7. Donsion, M. P., Guemes, J. A., & Rodriguez, J. M. (2007). Power quality benefits of utilizing FACTS controller. *IEEE Transactions*.
8. Omar, R., Rahim, N., & Suleiman, M. (2009). Modelling and simulation for voltage sag/swell mitigation using DVR. *Journal of Theoretical and Applied Information Technology*, 464-470.
9. Shakil, S., Srivastava, K. K., & Pandey, A. V. (2013). Power quality enhancement and sag mitigation by DVR. *International Journal of Science and Research*, 4(6).
10. Chankhamrian, W., Winittham, C., Bhumkittipich, K., & Manmai, S. (2014). Load side voltage compensation of small hydropower grid-connected system using DVR based on PV source. *Elsevier*.
11. Al-Mathnani, A. O., & Mohamed, A. W. (2007). Photovoltaic-based DVR for voltage sag mitigation. *SCORED*, 5.
12. Chankhamiran, W., & Bhumkittipich, K. (2011). The effect of series connected transformer in DVR application. *Eco-Energy and Materials Science and Engineering Symposium*.
13. Prakash, Y., & Sankar, S. (2015). Mitigation of voltage sag problem using DVR. *International Journal of Advanced Research in Engineering*, 4(10).
14. Bollen, M. H. J. (2000). *Understanding power quality problems: Voltage sags and interruptions*. IEEE Press.
15. IEEE. (1992). Recommended practice and recommendation for harmonics control in electric power systems. *IEEE Std 519*.
16. Salgado-Herrera, N. M., Medina Rioes, M., Tapia-Sanchez, A., Anaya-Lara, R., & Rodriguez, O. (2017). Sag and swell compensation and power factor correction using DVR in distribution system. *IEEE*.
17. Behera, M. P., & Ray, P. K. (2020). Reactive power and harmonic compensation in a grid-connected photovoltaic system using fuzzy logic controller. *International Journal of Emerging Electric Power Systems*, 22(2), 161-175. https://doi.org/10.1515/ijeeps-2020-0204
18. Behera, M. P., & Ray, P. K. (2015). Single-phase grid integrated photovoltaic inverter for harmonic and reactive power compensation. In *2015 Annual IEEE India Conference (INDICON)* (pp. 1-6). https://doi.org/10.1109/INDICON.2015.7443455
19. Behera, M. P., & Ray, P. K. (2019). Three-phase grid connected bi-directional charging system to control active and reactive power. *International Journal of Emerging Electric Power Systems*. https://doi.org/10.1515/ijeeps-2018-0259
20. Sahu, M. K., Malla, J. M. R., Biswal, M., & Behera, S. (2019). THD analysis and comparison of different cascaded multilevel inverters for improving the quality of energy. *International Journal of Applied Engineering Research*, 14(10), 2422-2429.
21. Behera, S., Dash, S. K., Sahu, M. K., Sahu, I., & Parida, S. (2023). Design and development of a new soft-switching buck converter. In *2023 International Conference on Power Electronics and Energy (ICPEE)* (pp. 1-6). IEEE. https://doi.org/10.1109/ICPEE54198.2023.10060126
22. Behera, S., Dash, S. K., Sahu, M. K., & Parida, S. (2022). Computation of maximum power point tracking of PV module using modified Newton-Raphson technique. *International Journal of Power Electronics and Drive Systems*, 13(4), 2478-2487. https://doi.org/10.11591/ijpeds.v13.i4.pp2478-2487
23. Mohanty, Monalisa, Niranjan Nayak, Bibhu Prasad Ganthia, and Manoj Kumar Behera. "Power Smoothening of Photovoltaic System using Dynamic PSO with ESC under Partial Shading Condition." In *2023 International Conference in Advances in Power, Signal, and Information Technology (APSIT)*, pp. 675-680. IEEE, 2023.
24. Kabat, Subash Ranjan, and Bibhu Prasad Ganthia, Chinmoy Kumar Panigrahi. "Fuzzy Logic and Synchronous Reference Frame Controlled LVRT Capability Enhancement in Wind Energy System using DVR." *Turkish Journal of Computer and Mathematics Education (TURCOMAT)* 12.6 (2021): 4899-4907
25. Xie, Hui, Yatao Wang, Zhiliang Gao, Bibhu Prasad Ganthia, and Chinh V. Truong. "Research on frequency parameter detection of frequency shifted track circuit based on nonlinear algorithm." *Nonlinear Engineering* 10, no. 1 (2021): 592-599.

26. Gu, Ji, Wang, Wei, Yin, Rong, Truong, Chinh V and Ganthia, Bibhu Prasad. "Complex circuit simulation and nonlinear characteristics analysis of GaN power switching device" *Nonlinear Engineering*, vol. 10, no. 1, 2021, pp. 555-562. https://doi.org/10.1515/nleng-2021-0046.
27. Sahu, P. K., Mohanty, A., Ganthia, B. P., & Panda, A. K. (2016, January). A multiphase interleaved boost converter for grid-connected PV system. In *2016 International Conference on Microelectronics, Computing and Communications (MicroCom)* (pp. 1-6). IEEE.
28. Ganthia, B. P., Barik, S. K., & Nayak, B. (2022). Genetic Algorithm Optimized and Type-I fuzzy logic controlled power smoothing of mathematical modeled Type-III DFIG based wind turbine system. *Materials Today: Proceedings*, *56*, 3355-3365.
29. Pahadasingh, S., Jena, C., Panigrahi, C. K., & Ganthia, B. P. (2022). JAYA Algorithm-Optimized Load Frequency Control of a Four-Area Interconnected Power System Tuning Using PID Controller. *Engineering, Technology & Applied Science Research*, *12*(3), 8646-8651.
30. Mishra, S., Ganthia, B. P., Sridharan, A., Rajakumar, P., Padmapriya, D., & Kaliappan, S. (2022). Optimization of load forecasting in smartgrid using artificial neural network based NFTOOL and NNTOOL. In *Journal of Physics: Conference Series* (Vol. 2161, No. 1, p. 012068). IOP Publishing.
31. Kabat, S. R., Panigrahi, C. K., & Ganthia, B. P. (2022). Comparative analysis of fuzzy logic and synchronous reference frame controlled LVRT capability enhancement in wind energy system using DVR and STATCOM. In *Sustainable Energy and Technological Advancements: Proceedings of ISSETA 2021* (pp. 423-433). Singapore: Springer Singapore.
32. Kumar, N., & Singh, B. (2021). Fuzzy logic-based MPPT control of a grid-connected PV system for power quality improvement. *IEEE Transactions on Industrial Informatics*, 17(4), 2498-2507.https://doi.org/10.1109/TII.2020.3017327
33. Mandal, P., Roy, B., & Chatterjee, D. (2020). Fuzzy logic controller-based power management in a hybrid PV-wind-grid connected microgrid system. *Renewable Energy*, 153, 203-215. https://doi.org/10.1016/j.renene.2020.01.084
34. Kermani, M., & Ghaffarzadeh, N. (2019). Design and implementation of a fuzzy logic-based controller for grid-connected PV systems to improve power quality. *Solar Energy*, 193, 436-445. https://doi.org/10.1016/j.solener.2019.09.061
35. Khare, M., & Singh, G. (2018). Fuzzy logic control strategy for grid integration of photovoltaic systems. *Energy Procedia*, 157, 1700-1706. https://doi.org/10.1016/j.egypro.2018.11.308
36. Sharma, D., & Singh, R. K. (2017). Fuzzy logic-based power quality improvement in grid-connected PV systems under variable solar conditions. *Journal of Power Electronics*, 17(4), 1060-1068. https://doi.org/10.6113/JPE.2017.17.4.1060
37. Patel, P., & Kumar, S. (2016). A fuzzy logic-based MPPT controller for grid-connected PV systems with power quality enhancement. *Journal of Electrical Engineering & Technology*, 11(2), 483-491. https://doi.org/10.5370/JEET.2016.11.2.483.
38. C. K. Barick, B. K. Mohapatra, S. R. Kabat, K. Jena, B. P. Ganthia and C. K. Panigrahi, "Review on Scenario of Wind Power Generation and Control," *2022 1st IEEE International Conference on Industrial Electronics: Developments & Applications (ICIDeA)*, Bhubaneswar, India, 2022, pp. 12-17, doi: 10.1109/ICIDeA53933.2022.9970193.
39. Rubavathy, S. J., Venkatasubramanian, R., Kumar, M. M., Ganthia, B. P., Kumar, J. S., Hemachandu, P., & Ramkumar, M. S. (2021, September). Smart Grid Based Multiagent System in Transmission Sector. In *2021 Third International Conference on Inventive Research in Computing Applications (ICIRCA)* (pp. 1-5). IEEE.
40. Zheng, W., Mehbodniya, A., Neware, R., Wawale, S. G., Ganthia, B. P., & Shabaz, M. (2022). Modular unmanned aerial vehicle platform design: Multi-objective evolutionary system method. *Computers and Electrical Engineering*, *99*, 107838.
41. A. Biswal, B. P. Ganthia, S. Satapathy, S. Patra, S. K. Bhatta and M. Mohanty, "Prototype Design of Modified Mechanical Drive Train Gear Box System using ANSYS for Wind Power Generation," *2022 Second International Conference on Artificial Intelligence and Smart Energy (ICAIS)*, Coimbatore, India, 2022, pp. 518-523, doi: 10.1109/ICAIS53314.2022.9743077.
42. Priyadarshini, L., Kundu, S., Maharana, M. K., & Ganthia, B. P. (2022). Controller Design for the Pitch Control of an Autonomous Underwater Vehicle. *Engineering, Technology & Applied Science Research*, *12*(4), 8967-8971.
43. Samal, S. K., Jena, S., Ganthia, B. P., Kaliappan, S., Sudhakar, M., & Kalyan, S. S. (2022). Sensorless Speed Contorl of Doubly-Fed Induction Machine Using Reactive Power Based MRAS. In *Journal of Physics: Conference Series* (Vol. 2161, No. 1, p. 012069). IOP Publishing.
44. Refaai, M. R. A., Dhanesh, L., Ganthia, B. P., Mohanty, M., Subbiah, R., & Anbese, E. M. (2022). Design and Implementation of a Floating PV Model to Analyse the Power Generation. *International Journal of Photoenergy*, *2022*.
45. Ganthia, Bibhu Prasad, et al. "Machine Learning Strategy to Achieve Maximum Energy Harvesting and Monitoring Method for Solar Photovoltaic Panel Applications." *International Journal of Photoenergy* 2022 (2022).